Available online at www.sciencedirect.com
SCIENCE DIRECT®
Journal of Pharmaceutical and Biomedical Analysis 38 (2005) 275–284
JOURNAL OF PHARMACEUTICAL AND BIOMEDICAL ANALYSIS
www.elsevier.com/locate/jpba

IR spectroscopy together with multivariate data analysis as a process analytical tool for in-line monitoring of crystallization process and solid-state analysis of crystalline product

Kati Pöllänen [a, b, *], Antti Häkkinen [a], Satu-Pia Reinikainen [b], Jukka Rantanen [c], Milja Karjalainen [d], Marjatta Louhi-Kultanen [a], Lars Nyström [a]

[a] *Lappeenranta University of Technology, Department of Chemical Technology, Laboratory of Separation Technologies, P.O. Box 20, 53851 Lappeenranta, Finland*
[b] *Lappeenranta University of Technology, Department of Chemical Technology, Laboratory of Analytical and Inorganic chemistry, P.O. Box 20, 53851 Lappeenranta, Finland*
[c] *Viikki Drug Discovery Center (DDTC), Pharmaceutical Technology Division, Department of Pharmacy, P.O. Box 56, University of Helsinki, 00014 Helsinki, Finland*
[d] *Pharmaceutical Technology Division, Department of Pharmacy, P.O. Box 56, University of Helsinki, 00014 Helsinki, Finland*

Received 17 August 2004; received in revised form 14 January 2005; accepted 14 January 2005
Available online 10 February 2005

Abstract

Crystalline product should exist in optimal polymorphic form. Robust and reliable method for polymorph characterization is of great importance. In this work, infra red (IR) spectroscopy is applied for monitoring of crystallization process in situ. The results show that attenuated total reflection Fourier transform infra red (ATR-FTIR) spectroscopy provides valuable information on process, which can be utilized for more controlled crystallization processes. Diffuse reflectance Fourier transform infra red (DRIFT-IR) is applied for polymorphic characterization of crystalline product using X-ray powder diffraction (XRPD) as a reference technique. In order to fully utilize DRIFT, the application of multivariate techniques are needed, e.g., multivariate statistical process control (MSPC), principal component analysis (PCA) and partial least squares (PLS). The results demonstrate that multivariate techniques provide the powerful tool for rapid evaluation of spectral data and also enable more reliable quantification of polymorphic composition of samples being mixtures of two or more polymorphs. This opens new perspectives for understanding crystallization processes and increases the level of safety within the manufacture of pharmaceutics.

Keywords: Controlled crystallization; In situ process monitoring; Multivariate analysis; Diffuse reflectance infra red spectroscopy; Attenuated total reflection infra red spectroscopy

1. Introduction

Desired polymorphic form of a crystalline product should be obtained and the product should be characterized quickly and reliably. Changes in a polymorphic form can influence the physical properties of a crystalline product, for example, mixing, milling and tabletting as well as the pharmaceutical performance of the crystalline product, for instance dissolution, stability and usability in the final dosage form [1]. Recently, the U.S. Food and Drug Administration (FDA) have addressed this issue by introducing draft guidance on process analytical technology (PAT) [2]. PAT is a system for developing and implementing new efficient tools for use during pharmaceutical development, manufacturing and quality assurance while maintaining or improving the current level of product quality assurance. This draft guideline categorizes PAT tools in four groups: multivariate data acquisition and analysis tools, modern process analyzers or process analytical chemistry tools, process and endpoint

* Corresponding author. Tel.: +358 5 621 2152; fax: +358 5 621 2199.
E-mail address: Kati.Pollanen@lut.fi (K. Pöllänen).

0731-7085/$ – see front matter © 2005 Elsevier B.V. All rights reserved.
doi:10.1016/j.jpba.2005.01.009

monitoring and control tools, and continuous improvement and knowledge management tools. Therefore, it is of critical importance to develop new approaches to increase the level of process understanding in pharmaceutical unit operations.

Cooling crystallization is an important purification unit operation. The supersaturation, which is defined by the difference between the solute concentration in ongoing crystallization process and the equilibrium concentration of the solute, is a driving force of the cooling crystallization process and an essential parameter to be monitored to control product properties, i.e., size distribution, habit and polymorphism. Attenuated total reflection Fourier transform infra red (ATR-FTIR) spectroscopy has been introduced for in situ concentration measurement in cooling crystallization processes [3–9]. In use of IR for concentration prediction purpose, the stable calibration is the most critical issue in order to have reliable concentration predictions. Multivariate partial least squares (PLS) calibration has been proved to be a suitable method for concentration prediction from spectral data in crystallization process monitoring applications [5–9]. In order to improve the multivariate calibration, spectra can be preprocessed. Traditional filtering methods applied are, e.g., multiplicative signal correction (MSC), Savitzky–Golay smoothing and standard normal variate (SNV) methods. However, it has been discussed by several authors that these methods may also remove information relevant to predicted variable. One approach is to utilize orthogonal signal correction (OSC) filtering methods to remove redundant or useless variation regarding modeled phenomena from the spectral data [10]. The calibration procedure with OSC preprocessing, data and model validation steps to predict solute concentration from crystallization processes using ATR-FTIR has been previously presented by authors [11].

The polymorphic composition of a solid material should be estimated. The product can be a mixture of two or more polymorphs. The fundamental method giving the structural information on a solid material is X-ray powder diffraction (XRPD). Additional technique is beneficial to confirm the estimation derived from XRPD measurements. Vibration spectroscopic techniques such as diffuse reflectance (DRIFT) and attenuated total reflection (ATR) in the mid-FTIR bandwidth as well as NIR have previously been applied in polymorph characterizations [12–16].

The multivariate principal component analysis (PCA) and partial least squares regression methods are powerful when spectral data is modeled or interpreted. PCA has been applied by Aaltonen et al. [15] for rapid screening of sulfathiazole crystals measured with NIR. PCA based multivariate statistical process control (MSPC) charts are widely used in quality measurements in process industry, but those could also be applied for crystalline sample purity analyses from spectral data. PLS is suitable for quantitative predictions of sample composition from spectral data.

In this study, sulfathiazole was used as a model compound. Its polymorphism has been studied widely [17–20]. Sulfathiazole is known to have at least four polymorphic forms. Crystallizing sulfathiazole, especially from solvent mixtures, may result in a single polymorph form or mixtures of two or more polymorphs [20].

In this study, sulfathiazole was crystallized from five different mixtures of water and 1-propanol using four different constant cooling rates. ATR-FTIR was applied for in situ concentration measurement to be able to evaluate concentration level effects to outcome of product. Further, the polymorphic compositions of obtained solid-state samples were characterized using XRPD and DRIFT. Estimations of polymorphic composition were carried out by correlating calculated XRPD diffractograms from Cambridge Crystallographic Data Center (CCDC) to the XRPD measurements from samples. Multivariate PCA and MSPC analyses were applied and found suitable for analyzing DRIFT data, since with these methods the samples are easy to classify based on the dominant polymorph in the sample, abnormal samples can be detected and quality of the samples evaluated. Applying PLS analysis to the DRIFT spectra and to results from XRPD analysis confirmed the quantification made by XRPD and allowed polymorphic composition predictions to be made from DRIFT data.

2. Materials and methods

2.1. Crystallization experiments

The batch cooling crystallization experiments on sulfathiazole were performed in a 4-l jacketed mixing tank equipped with four baffles, a 3-bladed propeller, a condenser and a programmable Lauda RK 8 KP thermostat. Pt-100 sensor was used to measure solution temperature inside the crystallizer and measurement data was collected onto a PC. The mixing speed used in all the experiments was 400 rpm. The experimental set up is presented in Fig. 1.

Sulfathiazole (Industrias GMB, Spain) was crystallized from water, 1-propanol and aqueous 1-propanol of 50/50, 25/75 and 75/25 wt%. Deionised water and European Pharmacopoeia/United States Pharmacopoeia (EP/USP) grade 1-propanol (Labscan Ltd., Ireland) were used in the solvent mixture. The suspension was cooled from 80 to 25 °C at constant cooling rates of 27.5, 9.2, 5.5 and 3.9 °C/h. The amount of dissolved sulfathiazole corresponded to the solubility in the particular solvent at 80 °C and were 0.9, 2.2, 20.6, 15.8, 10.9 g sulfathiazole/100 g solvent for water, 1-propanol, 50/50, 25/75 and 75/25 wt% mixtures, respectively.

2.2. In situ attenuated total reflection Fourier transform infra red concentration measurements

The absorbance spectrum was collected from crystallizer in situ with BOMEM MB155S spectrophotometer equipped with Axiom Analytical Dipper 210 ATR immersion probe. ZnSe was used as a reflecting element. Wave number range from 4000 to 750 cm^{-1} was measured. Spectral resolution

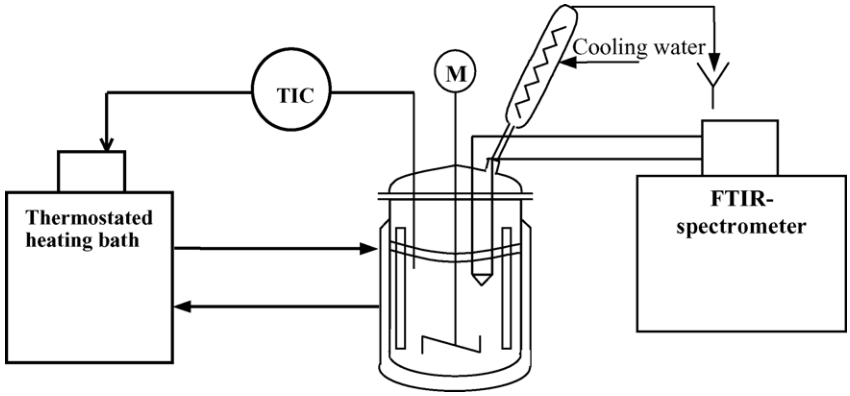

Fig. 1. Crystallization set up.

used was 16 cm^{-1} and number of scans 20. Those settings were found to be a good compromise between the signal to noise ratio and robustness of the measurements. The spectrum was collected with time increments of a minute during the whole crystallization process.

2.2.1. Calibration measurements

The absorbance spectrum is transformed to the information on concentration by deriving a calibration model. The set of samples with known compositions were measured as close as possible to the conditions where true measurements took place. The spectral responses were correlated to composition by PLS modeling. Sulfathiazole concentration from 0 to 30 g sulfathiazole/100 g solvent and solvent composition 0–100 wt% 1-propanol was covered in calibration measurements. Detailed description of the calibration measurements is presented in [11].

2.3. Crystal size characterization

Crystal size distributions were obtained using an automated image analyzer (PharmaVision 830, Malvern Instruments Ltd.). Sulfathiazole crystals were dispersed evenly on a 100 mm × 100 mm sample plate that was placed on a sample tray underneath a video camera. The camera was moved across the sample tray stepwise, and a large set of digitized video images was automatically acquired. PharmaVision 830 software (version 4.2.1.15) was used to process the images by separating all the individual crystals and determining size parameters for each crystal in the sample.

2.4. Diffuse reflectance Fourier transform infrared (DRIFT-IR) measurements

The aim of the DRIFT measurements was to find robust way to estimate the polymorphic composition of the crystalline bulk material. The samples were measured using a Perkin-Elmer IR spectrometer accompanied with a diffuse reflectance accessory. Grinded KBr powder was used as the background in the measurements. Sulfathiazole samples were ground before measurement in order to increase relative reflectance coming out of samples. Spectral resolution used was 8 cm^{-1} and number of scans was 10. From two to five parallel secondary samples from each primary sample were measured.

2.5. X-ray powder diffraction measurements

The ground sulfathiazole crystals were measured using a German-made X-ray powder diffractometer Bruker axs D8. The X-ray diffraction experiments were performed in symmetrical reflection mode with Cu Kα radiation (1.54 Å) using Göbel Mirror bent gradient multilayer optics. The scattered intensities were measured using a scintillation counter. The angular range was from 5° to 40° with steps of 0.05° and a measuring time of 1 s/step. The XRPD patterns measured were compared to theoretical patterns generated on the basis of data obtained from CCDC with Cerius^{2TM} (Diffraction-Crystal module; Accelrys Inc., Cambridge, UK).

2.6. Mathematical methods applied for spectral data

The spectral data was analyzed using Matlab 6.5 from the MatWorks Inc. Calibration modeling for both (a) concentration predictions from in situ ATR-FTIR measurements and (b) the data processing for DRIFT spectra were done as follows: the quality of the data was evaluated before and afterwards the pre-processing operations using PCA and MSPC. The samples included in the calibration set were selected based on data evaluation and previous knowledge on the variables. Spectra were preprocessed by filtering or/and variable selection to improve the model performance. PLS model with proper number of dimensions was derived and the model was validated using external test set. Detailed explanation of calibration routines applied in this context is described in [12].

2.6.1. PCA and MSPC analyses

PCA and MSPC charts were applied to the mean-centered data before and after the preprocessing. The purpose of this treatment was to find outliers and disturbing regions within

the spectra, to investigate the sample clustering when the structure is interpreted, and to ascertain that the applied pretreatment did not remarkably distort the data structure.

In PCA, the data matrix (**X**) is decomposed as follows:

$$\hat{\mathbf{X}} = \sum_{i=1}^{A} \mathbf{t}_i \mathbf{p}_i^{\mathrm{T}} + \mathbf{E}$$

where **t** is the score vector that represent the scaling coefficients of the samples and can be used to cluster samples to different groups and represent the structure, and **p** are loadings that represent the most dominant spectral variations and can be used to find, e.g., the most important variables in the variable space. **E** is residual that is considered 'noise'.

MSPC analysis is based on PCA. Hotelling's T^2 charts accompanied to T^2 contribution charts are formed from score vectors. T^2 is calculated by:

$$T_A^2 = \sum_{i=1}^{A} \frac{\mathbf{t}_i^2}{\mathbf{s}_{\mathbf{t}_i}^2}$$

where $\mathbf{s}_{\mathbf{t}}^2$ is the estimated variance of $\mathbf{t}_i$.

T^2 represents the data structure of a particular sample corresponding to the data structure in the model. Q chart and Q contributions are detected from squared prediction error of the residuals of observation:

$$Q = \sum_{i=1}^{k} (\mathbf{x}_{\mathrm{new},i} - \hat{\mathbf{x}}_{\mathrm{new},i})$$

By T^2 and Q charts somehow extreme samples either in the model or in the residual space can be found. Contribution charts visualize the variables in the model (T^2) and residual (Q) space. By this way, the most important or the most 'disturbing' variables within spectra can be pointed out and possible variable selection applied. The theoretical bases of these methods are represented in, e.g., Vandeginste et al. [21].

2.6.2. Partial least squares model

The PLS is a commonly used method to obtain predictive model from collinear data, type which the spectral data obviously represent. The PLS models can have several advantages compared to ordinary regression methods. (1) In PLS, the collinearity between variables represents a stabilizing advantage rather than a problem, which is the case in the ordinary regression. (2) The number of objects does not restrict the number of wave numbers used in modelling. (3) PLS can be used to reduce the dimensions of the original data and, at the same time, it may reduce the noise level in the data. In partial least squares regression, the **Y** and **X** matrices are decomposed into the structure and noise parts. A score vector **t** in the column space of **X** (**t** = **Xw**) and a vector **u** in a column space of **Y** (**u** = **Yq**). Vectors **t** and **u** are fitted in order to give the maximal squared covariance:

$$\max(\mathbf{u}'\mathbf{t})^2 = \max(\mathbf{q}'\mathbf{Y}'\mathbf{X}\mathbf{w})^2 \quad \text{for } |\mathbf{w}| = |\mathbf{q}|$$

where **w** and **q** are loadings of the **X** and **Y** decompositions, respectively. Several such derived components can be calculated. The mathematical formulation that describes the PLS approach is discussed, for instance, in [22].

2.6.3. Processing the ATR-FTIR spectra for in situ solute concentration prediction in crystallization process

In the ATR-FTIR concentration measurement, the **X** matrix consists of the spectral variables, temperature and solvent composition and the **Y** variable is sulfathiazole concentration to be predicted. The temperature and solvent composition variables were scaled to the level of spectral variations and whole **X** data was centered.

Data preprocessing was applied in order to enhance the calibration model interpretability and performance. The aim in preprocessing is to remove information that hinders predictive ability of the modeling. The orthogonal signal correction (OSC) preprocessing methods were developed for removing systematic variation in **X** that is not correlated to **Y** by ensuring that the information removed from data matrix **X** is mathematically orthogonal to **Y**. In OSC filtering the single component 'OSC model' is built:

$$\mathbf{X} = \mathbf{t}_{\mathrm{OSC}} \mathbf{p}_{\mathrm{OSC}}^{\mathrm{T}} + \mathbf{E}, \qquad \mathbf{t}_{\mathrm{OSC}} = \mathbf{X}\mathbf{w}_{\mathrm{OSC}}, \qquad ||\mathbf{x}_{\mathrm{OSC}}|| = 1$$

where $\mathbf{t}_{\mathrm{OSC}}$, $\mathbf{p}_{\mathrm{OSC}}$ and $\mathbf{w}_{\mathrm{OSC}}$ are scores and loadings of OSC component similar to the PLS components, but the score vectors ($\mathbf{t}_{\mathrm{OSC}}$) are orthogonal to **Y**. Matrix **E** one OSC component filtered data matrix. If more OSC components are to be filtered from the data, the filter is applied to **E**. Eventually, **E** is the filtered matrix to be used in, e.g., PLS calibration [9]. Several authors have derived different approaches to OSC, e.g., [9,23–27]. Methods differ from each other by the way the orthogonal score vectors are found [23]. In present predictive model, OSC filter introduced by Höskuldsson [25] (denoted $\mathrm{OSC_{AH}}$) and by Wold et al. [23] (denoted $\mathrm{OSC_{SW}}$) were applied and tested. The proper filtering procedure and number of PLS components were validated using an external test set. This resulted in 2-dimensional PLS model derived from four OSC components filtered data. The close description of the calibration procedure is presented in [11]. The best performing model is selected based on the root mean squared error of validation (RMSEV) of the test set:

$$\mathrm{RMSEV} = \left(\frac{\sum (y_i - \hat{y}_i)^2}{n_i} \right)^{1/2}$$

where y_i is measured and $\hat{y}_i$ predicted response value and n_i is number of samples. RMSEV for the test set is suitable for describing the true performance of the predictive model since it gives estimation on prediction accuracy of the new samples. In practice, a convergence criteria, presented in [21] is applied for RMSEV values to select the stable model with low RMSEV value that gives accurate enough predictions but the over fitting is avoided.

2.6.4. Processing the DRIFT and XRPD data of crystalline samples

The quantification of polymorphic composition of the samples was based on the assumption that the experimental XRPD intensity curve is a linear combination of the intensity of polymorphic components. The crystal structures of the polymorphic forms were estimated by fitting the simulated intensity curves of the sulfathiazole polymorphic components to the experimental diffraction curve of sample. The amount of a component was calculated as the ratio of the integrals related to the intensities of the component and the studied sample [14]. The simulated sulfathiazole forms SUTHAZ01, SUTHAZ02, SUTHAZ and SUTHAZ05 (CCDC refcodes) were used as the polymorphic components.

In DRIFT measurement, the **X** matrix consists of the spectral variables and the **Y** matrix is the polymorphic compositions of SUTHAZ01, SUTHAZ02, SUTHAZ and SUTHAZ05 estimated from XRPD data for the samples (estimation described in following section). After data quality evaluation, the proper calibration set for PLS model was selected to have all variation represented but exclude the outlier samples.

Several **Y** variables can be combined to one single model if **Y** variables are correlated with each other. If a descriptor phenomenon of the variables is different, it is preferable to model each of the **Y**s separately. In this study, the correlation coefficients between the compositions of SUTHAZ01, SUTHAZ02 and SUTHAZ05 were appropriately high (above 0.7) and those could be modeled by the single PLS model, but the correlation of SUTHAZ to other polymorph compositions was too low to be included in the single model.

Based on the investigation of the variables from MSPC the most important variable range appeared to be the ones from 3700 to 2800 cm^{-1}, and this range was selected as the **X** variable range.

When measuring powdered solids with diffuse reflectance, the light scattering off the particles can cause irregular variation to the spectrum. These differences can be caused by the variation in the particle size or the alignment of the incident beam of light [28]. In this context, standard normal variation (SNV) [28] correction is used. SNV corrected spectrum is

$$A_{i(\mathrm{SNV})} = \frac{A_i - \bar{a}_i}{\sqrt{\frac{\sum_{j=1}^{p}(A_{i,j}-\bar{a}_i)}{(p-1)}}}$$

where A is the $n \times p$ matrix of training set spectral responses for all the wavelengths, i the single measurement, n number of samples, p number of variables within the spectrum and $\bar{a}_i$ is the average of all the spectral responses in the vector. SNV attempts to correct the effects of light scattering and the particle size was found to improve the data for multivariate modeling purposes [28].

The PLS model was applied for the SNV treated data and the proper number of PLS components was selected based on cross validation criteria, which was done by recalculating the model by leaving samples out and evaluating how these left out samples affect the model. In addition, external test set was used to validate the model.

3. Results and discussion

3.1. Concentration prediction from in situ ATR-FTIR measurements and their influence on crystal size and habit

Calibration model OSC- and PLS factor selection principles in calibration model and evaluation of performance of selected models is illustrated in Fig. 2.

Development of root mean squared errors of validation (RMSEV) values from 1 to 5 PLS component PLS models for differently pre-treated data is illustrated in Fig. 2a. The RMSEV value after the first PLS component in the model is clearly lower after OSC filtering has been applied, than without OSC filtering. Also, in order to obtain best performing model in terms of RMSEV values number of PLS components needed in the model is lower

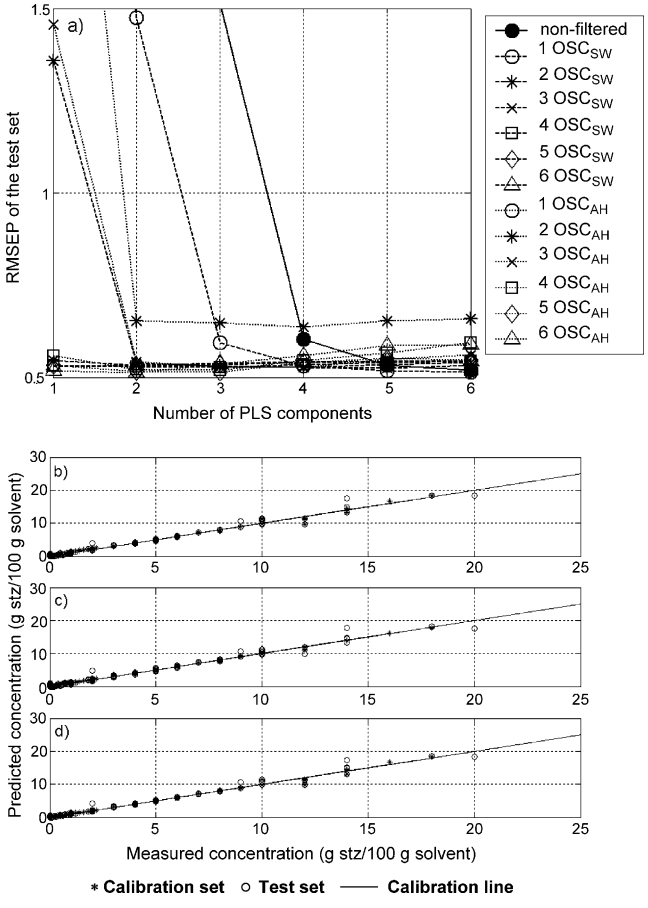

Fig. 2. ATR-FTIR calibration model. (a) Root mean squared error of prediction for the test set for the models derived from non-filtered, OSC_{sw} filtered and OSC_{AH} filtered data. Observed vs. predicted concentrations from (b) 5-component PLS model from non-filtered data, (c) 2-component PLS model from OSC_{SW} filtered (2-comp.) data, (d) 2-component PLS model from OSC_{AH} filtered (3-comp.) data.

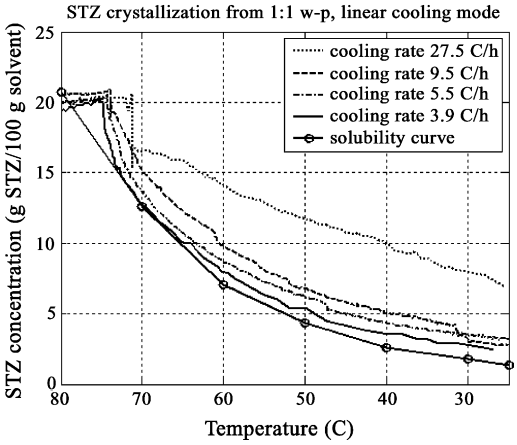

Fig. 3. The concentration profiles from cooling crystallization process with four different cooling rates.

for the model derived from OSC filtered data than a model built-up from non-filtered data (Fig. 2a). The observed concentrations versus predicted concentrations using three models derived from three differently pre-treated calibration data are presented in Fig. 2b–d. It can be seen that the prediction accuracy is sufficient for all compared models and differences are only of a minor scale. However, comparison of the residuals in observed versus predicted revealed that the OSC_{AH} performed slightly the best.

Concentration profiles were measured from all crystallizations to characterize the role of cooling on outcome of sulfathiazole crystals. Sudden decrease in concentration in the beginning of crystallization process indicates the primary nucleation, i.e., the metastable limit was exceeded at that point (Fig. 3).

The decrease in concentration level was remarkable in these experiments because only spontaneous nucleation took place. With seed crystals the onset of crystallization is usually less drastic. The width of the metastable zone became wider as the cooling rate increased being as it narrowest at 5 °C (80–75 °C) with 3.9 °C/h cooling rate and the widest at 8 °C (80–72 °C) with 27.5 °C/h cooling rate.

With the highest cooling rate, 27.5 °C/h, the predicted supersaturation was extremely high (Fig. 3). Also, the broadest size distribution of crystals and the most irregular shaped crystals were obtained with 27.5 °C/h cooling rate (Fig. 4). The concentration level was most likely high enough to exceed metastable limit throughout the crystallization with 27.5 °C/h cooling rate. This caused the solution cool down faster than the solute could transfer onto existing crystals, and consequently the spontaneous nucleation took place throughout the process.

The concentration level lowered significantly when cooling rate decreased from 27.5 to 3.9 °C/h (Fig. 3). Most likely the level of primary nucleation during the crystallization was small with cooling rates from 9.2 to 3.9 °C/h since also the size distribution became narrower than with cooling rate of 27.5 °C/h. With 3.9 °C/h cooling rate, however, influence of attrition of crystals may have become greater, since the size distribution is slightly broader than with cooling rates of 9.2 or 5.5 °C/h. (Fig. 4)

On the reliability of the predictions, the process conditions differed both chemically (the highest supersaturation) and physically (new crystals forming throughout the process) from the calibration measurements remarkably when the highest, 27.5 °C/h, cooling rate was used. Therefore, the predictions from that crystallization experiment are the most uncertain of all crystallizations; predicted values are probably higher than true values. However, the trend of increasing supersaturation compared to other crystallizations can be investigated. With other cooling rates from 9.2 to

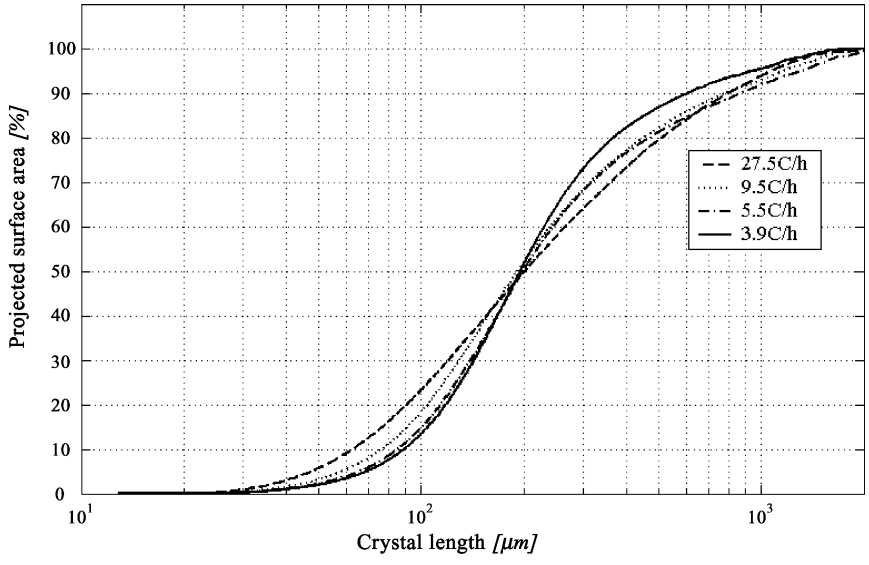

Fig. 4. Cumulative size distributions of the product crystals from sulfathiazole crystallizations using four different cooling rates.

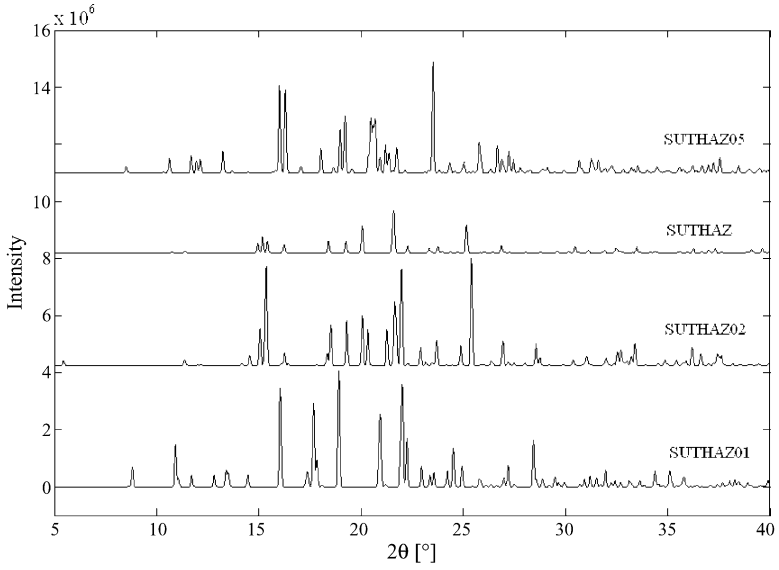

Fig. 5. References of the X-ray diffraction patterns of polymorphs of sulfathiazole.

3.9 °C/h, the process conditions were close to the calibration measurements as well as close to the values of the validation procedure [20]. Therefore, the predictions from those measurements can be considered reliable not only by trend but also the true concentration value.

3.2. Polymorph characterization

3.2.1. XRPD patterns

The theoretical XRPD patterns (CCDC) of sulfathiazole polymorphs are presented in Fig. 5.

Table 1
Compositions of sulfathiazole samples

Sample	XRPD results				Calibration set			Test set		
Polymorph: SUTHAZ	01	02		05	01	02	05	01	02	05
Bulk	0.2	0.5	0.2	0.1	0.21 ± 0.01	0.51 ± 0.01	0.09 ± 0.01	0.17 ± 0.01	0.54 ± 0.01	0.08 ± 0.01
P25W75A	0.2	0.8	0	0	0.24 ± 0.04	0.67 ± 0.03	n.d.	0.23 ± 0.05	0.73 ± 0.05	n.d.
P25W75A	0.3	0.7	0	0	0.27 ± 0.05	0.69 ± 0.01	n.d.	0.24 ± 0.03	0.73 ± 0.02	n.d.
P25W75B	0.2	0.6	0.2	0	0.22 ± 0.04	0.67 ± 0.01	n.d.	0.17 ± 0.05	0.69 ± 0.05	n.d.
P25W75C	0.2	0.6	0.2	0	0.24 ± 0.05	0.67 ± 0.04	n.d.	0.18 ± 0.02	0.71 ± 0.04	n.d.
P25W75D	0.3	0.6	0.1	0	0.30 ± 0.05	0.65 ± 0.04	n.d.	0.27 ± 0.00	0.71 ± 0.01	n.d.
P25W75D	0.3	0.7	0	0	0.36 ± 0.05	0.70 ± 0.04	n.d.	0.25 ± 0.05	0.71 ± 0.05	n.d.
P50W50A	0.2	0.6	0.2	0	0.26 ± 0.02	0.66 ± 0.04	n.d.			
P50W50A	0.2	0.7	0.1	0	0.22 ± 0.02	0.70 ± 0.04	n.d.	0.19 ± 0.04	0.73 ± 0.02	n.d.
P50W50B	0.2	0.7	0.1	0	0.23 ± 0.04	0.66 ± 0.00	n.d.	0.23 ± 0.05	0.71 ± 0.05	n.d.
P50W50C	0.4	0.6	0	0	0.30 ± 0.05	0.70 ± 0.04	n.d.	0.30 ± 0.05	0.75 ± 0.05	n.d.
P50W50D	0.2	0.7	0.1	0	0.20 ± 0.05	0.70 ± 0.04	n.d.	0.20 ± 0.04	0.73 ± 0.04	n.d.
P50W50D	0.2	0.8	0	0	0.25 ± 0.07	0.70 ± 0.03	n.d.	0.24 ± 0.09	0.75 ± 0.00	n.d.
P75W25A	0.1	0.8	0.1	0	0.15 ± 0.05	0.75 ± 0.04	n.d.	0.14 ± 0.05	0.79 ± 0.05	n.d.
P75W25A	0.3	0.7	0	0	0.28 ± 0.09	0.67 ± 0.04	n.d.	0.25 ± 0.07	0.72 ± 0.05	n.d.
P75W25B	0.3	0.6	0.1	0	0.28 ± 0.03	0.65 ± 0.01	n.d.	0.20 ± 0.05	0.72 ± 0.05	n.d.
P75W25C	0.2	0.7	0.1	0	0.21 ± 0.00	0.69 ± 0.03	n.d.	0.19 ± 0.05	0.75 ± 0.05	n.d.
P75W25C	0.2	0.7	0.1	0	0.20 ± 0.05	0.73 ± 0.05	n.d.			
P75W25D	0.2	0.7	0.1	0	0.22 ± 0.04	0.70 ± 0.06	n.d.	0.20 ± 0.12	0.73 ± 0.06	n.d.
P75W25D	0.4	0.6	0	0	0.31 ± 0.05	0.70 ± 0.04	n.d.	0.26 ± 0.05	0.76 ± 0.05	n.d.
PA	0.7	0.1	0	0.2	0.70 ± 0.06	0.11 ± 0.08	0.20 ± 0.00	0.64 ± 0.05	0.17 ± 0.04	n.d.
PD	0.7	0.2	0	0.1	0.68 ± 0.14	0.20 ± 0.22	0.11 ± 0.14	0.71 ± 0.05	0.15 ± 0.16	n.d.
PD	0.7	0.1	0	0.2				0.68 ± 0.11	0.24 ± 0.06	n.d.
WA	0.2	0.7	0.1	0				0.18 ± 0.01	0.75 ± 0.01	n.d.
WD	0.3	0.7	0	0	0.31 ± 0.05	0.66 ± 0.04	0.02 ± 0.02	0.28 ± 0.05	0.71 ± 0.05	n.d.

Mean estimated level of confidence of estimated compositions based on XRPD measurements ± 0.1. Sample names consist on solvent composition, P, 1-propanol, W, water and numbers behind the letters represent percentage composition in solvent and cooling rate is represented in the final letter, A = 27.5 °C/h, B = 9.5 °C/h, C = 6.5 °C/h, D = 3.9 °C/h.

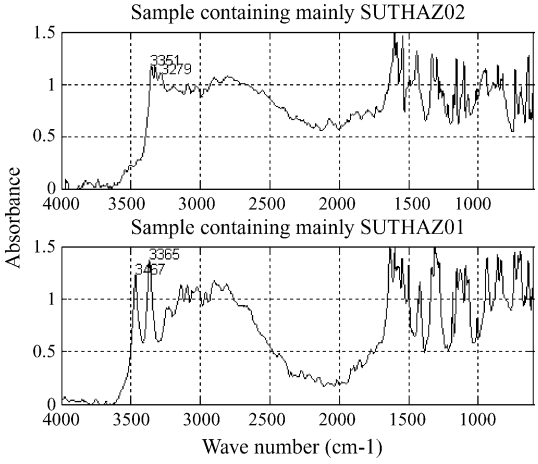

Fig. 6. Example DRIFT spectra.

These diffraction patterns were used as reference values in estimation of polymorphic composition of the samples. XRPD patterns from samples revealed that the samples crystallized from pure 1-propanol represented mostly SUTHAZ01 and ones crystallized from water or aqueous 1-propanol represented mostly SUTHAZ02. However, most of the samples were more or less mixtures of two or more polymorphs as is illustrated from quantification result in Table 1.

3.2.2. DRIFT spectra

Example spectra of sulfathiazole solid-state samples in Fig. 6 illustrate that the visible difference in the spectrum lies within the wave number range from 3500 to 3250 cm^{-1}.

There are two intense characteristic bands at 3467 and 3365 cm^{-1}in the spectrum obtained from sample containing mostly SUTHAZ01 that do not occur in the spectrum measured from sample containing mostly SUTHAZ02. The spectra from samples containing mostly SUTHAZ02, but also different fractions of other polymorphs, represent the slight differences compared to example spectrum in Fig. 6: the variation in ratio of bands in 3351 and 3279 cm^{-1} is different when the minor polymorph composition changes. Consequently, the polymorphic composition of samples could be studied further by multivariate analysis within the spectral range from 3500 to 2500 cm^{-1}. The primary analysis of covariance confirmed this being the most relevant spectral band range for analysis purposes. There is also lot of information in spectral range from 1800 to 600 cm^{-1}, but the relation to the polymorph composition seems to be more apparent in the range of 3500–2500 cm^{-1} in terms of multivariate analysis.

3.2.3. MSPC analysis of DRIFT spectra

MSPC charts are visualized in Fig. 7.

Upper left corner of Fig. 7 visualizes how the samples are located within the model (T^2 chart) and 95% limit line is presented. Upper right hand corner of Fig. 7 visualizes the 95% confidence levels for the variables within the model and the variables of example sample in that chart (T^2 contributions). Most of the samples lied within the 95% confidence limit in the T^2 chart in Fig. 7. The samples exceeding the confidence limit were the ones crystallized from pure 1-propanol and represent SUTHAZ01 based on XRPD. It could be seen from T^2 contributions in Fig. 7 that the spectral range where these samples exceeded the confidence limit was the area where two intense bands typical for SUTHAZ01 were located. MSPC charts proved to be capable for determining which polymorph the particular sample represent. Lower left corner of Fig. 7 represents the residuals of the samples (Q chart), i.e., how the samples are located in residual space. Lower right corner represents 95% confidence limits of the variance of the data that is left in the residuals (Q contributions). In Q chart, some samples represent unexceptional baseline behavior as is seen in Q contribution chart. Therefore, MSPC

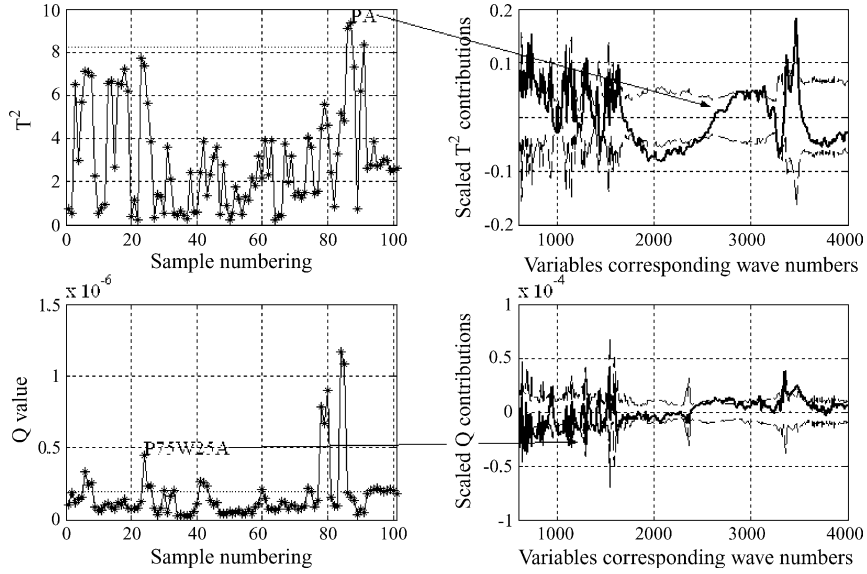

Fig. 7. MSPC charts of the DRIFT data.

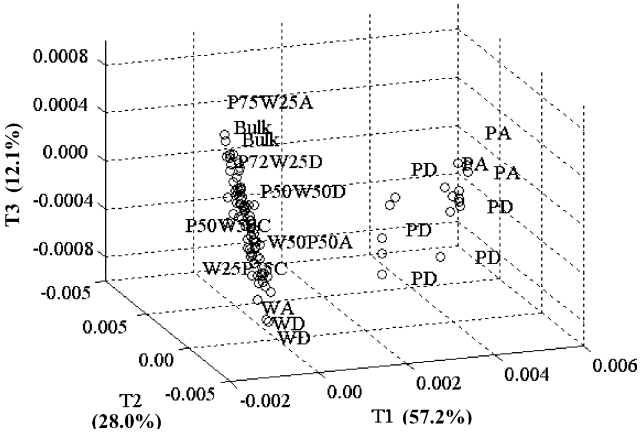

Fig. 8. Score vectors of PCA analysis of the DRIFT spectra. Percentage of variation explained (R^2) by a particular score vector is represented in parenthesis.

charts were powerful in determining also possible errors within the measurement procedure.

Generally speaking, MSPC illustrates whether or not particular sample represents similar data structure than the other samples and also which variables, i.e., spectral points cause these samples to be different. In practice, the samples representing polymorphs different than modeled ones can be separated. However, to distinguish between the samples being erroneous measurements or sample representing phenomenon different than the average modeled samples do, knowledge on the samples and their properties or extended data set is needed.

3.2.4. PCA score vectors of DRIFT spectra

From the three first score vectors of PCA plotted in Fig. 8, it can be observed that samples tend to cluster into two main groups.

The first group consisted of the samples that were crystallized from 1-propanol (PD and PA) representing mainly SUTHAZ01 based on XRPD. The other group consisted of the samples crystallized from solvents containing water and main component according to XRPD was SUTHAZ02. In bigger cluster (Fig. 8), the samples from water (WA and WD) the most pure SUTHAZ02 samples lied in the bottom and the bulk samples (Bulk), which were the most impure samples at the top of the group.

PCA provides illustrative tool to separate samples based on their main polymorph component. In addition, PCA indicates whether or not there is systematic trend in how the samples settle within the cluster in the space of score vectors and that could lead to the possibility to separate also small-scale changes within the sample composition.

3.2.5. PLS analysis

The results of PLS analysis of the samples are represented in Table 1. XRPD results for polymorphs SUTHAZ01, SUTHAZ02, SUTHAZ and SUTHAZ05 were used as observed values in columns from two to five, and the compositions predicted from DRIFT spectra for the calibration set and test set are represented in columns from 6 to 10. As mentioned in Section 2.4.1, SUTHAZ01, SUTHAZ02 and SUTHAZ05 could be modeled by the single PLS model and the PLS modeling results exist only for these three polymorphs.

It can be observed that concentration predictions for both calibration and test sets are consistent with XRPD results. Main components SUTHAZ01 and SUTHAZ02 can be predicted with appropriate accuracy compared to accuracy of XRPD predictions. Also, the small fractions of SUTHAZ05 can be distinguished from DRIFT data via PLS analysis, which indicates that actual differences exist within the data when sample contains even small fractions of SUTHAZ05 to that when this polymorph does not exist.

The prediction result is strongly restricted by the fact that the accuracy of the reference values out of XRPD results is rather low. The predictions obtained when using PLS model, can be said to give encouraging results, since variances of the predictions of parallel DRIFT samples are rather low and, despite of the high uncertainty of reference XRPD values, the compositions predicted using PLS model compromise fairly well to observations, i.e., to XRPD results.

3.2.6. Process condition effects on polymorphic outcome

Theoretically, the level of supersaturation could influence in the polymorphic outcome of the crystals due to the fact that solubilities of the specific polymorphs to the particular solvent are different [1]. In principle, if the cooling takes place at concentration level that lies between the solubility of two polymorphs, the polymorph with lower solubility should appear. If the concentration level could be carefully controlled, it might be possible to control the polymorphic outcome of product crystals. Obtaining a product that would contain the desired polymorph only is complicated by the stepwise conversion between different forms. As stated by Ostwald's law, a metastable polymorph will eventually undergo a phase transformation to a more stable one, and finally to the thermodynamically most stable form. In addition, the formation of polymorphs can be driven by several different factors in crystallization; one being the solvent composition and the most dominant factor is not unambiguously resolved by the time being [1].

In this study, polymorphic composition of the product crystals seemed not to depend on the cooling rate used although the concentration levels in crystallization were remarkably different (Fig. 3), but the polymorph compositions of product crystals crystallized from certain solvent were almost equal. This can be due to the fact that differences in solubilities of different sulfathiazole polymorphs for example in 1-propanol are rather small [17]. As was previously mentioned, the dominant effect for the polymorphic outcome of crystals appeared to be the solvent composition

and more specifically whether or not the solvent contained water.

4. Conclusions

Sulfathiazole was crystallized from five aqueous 1-propanol mixtures using four different constant cooling rates. Attenuated total reflection Fourier transform infra red was applied for in situ concentration measurement. The obtained crystals were characterized using X-ray powder diffraction and diffuse reflectance Fourier transform-infra red. Estimations of polymorphic composition were carried out by correlating theoretical reference diffractograms from CCDC to the samples measured with XRPD. Principal component analysis, multivariate statistical process control charts and partial least squares modeling techniques were introduced to analyze DRIFT data for polymorph characterization.

ATR-FTIR technique gave a possibility to evaluate concentration level effects on product properties and that was found to be significant for size and shape of product crystals but not for polymorphic outcome. Polymorphic outcome seemed to be driven by solvent composition and more specifically whether or not the solvent contained water. The XRPD results revealed that the product crystals were mixtures of two or more polymorphs main component being SUTHAZ01 when crystallized from 1-propanol and SUTHAZ02 when crystallized from water or aqueous 1-propanol.

MSPC and PCA methods provided simple and powerful tools to evaluate the quality of crystalline samples from DRIFT spectra, since the samples could easily be classified based on the dominant polymorph in the sample and abnormal samples could be detected. PLS analysis applied to the DRIFT spectra and to results from XRPD analysis confirmed the quantification made by XRPD and allowed polymorphic composition predictions made from DRIFT data, which provides complementary method for polymorph characterization.

Acknowledgements

Orion Corporation Orion Pharma, National Technology Agency of Finland and Academy of Finland are acknowledged for financial support. Ms. Päivi Hovila is kindly acknowledged for performing the DRIFT measurements.

References

[1] H.G. Brittain (Ed.), Polymorphism in Pharmaceutical Solids, Drugs and the Pharmaceutical Sciences, vol. 95, Marcel Dekker Inc., NY, 1999.
[2] PAT—a Framework for Innovative Pharmaceutical Manufacturing and Quality Assurance; U.S. Food and Drug Administration (FDA), Rockville MD, USA, 2003.
[3] M. Uusi-Penttilä, K.A. Berglund, J. Cryst. Growth 166 (1996) 967–970.
[4] F. Lewiner, G. Fevotte, J.P. Klein, F. Puel, J. Cryst. Growth 226 (2001) 348–362.
[5] H. Groen, K.J. Roberts, J. Phys. Chem. 105 (2001) 10723–10730.
[6] L. Feng, K.A. Berglund, Cryst. Growth Des. 2 (2002) 449–452.
[7] T. Togkalidou, M. Fujiwara, S. Patel, R.D. Braatz, J. Cryst. Growth A 231 (2001) 534–543.
[8] V. Profir, E. Furusjö, L.-G. Danielsson, Å.C. Rasmuson, Cryst. Growth Des. 2 (2002) 273–279.
[9] K. Pöllänen, A. Häkkinen, S.-P. Reinikainen, M. Louhi-Kultanen, L. Nyström, Proc. Suppl. Vol. ESCAPE 13 (2003) 93–99.
[10] S. Wold, H. Antti, F. Lindgren, J. Öhman, Chemom. Intell. Lab. Syst. 44 (1998) 175–185.
[11] K. Pöllänen, A. Häkkinen, S-P. Reinikainen, M. Louhi-Kultanen, L. Nyström, Chemom. Intell. Lab. Syst., in press.
[12] R. Helmy, G.X. Zhou, Y.W. Chen, L. Crocker, T. Wang, R.M. Wenslow Jr., A. Wailaya, Anal. Chem. 75 (2003) 605–611.
[13] A. Salari, R.E. Young, Int. J. Pharm. 163 (1998) 157–166.
[14] K. Dohi, F. Kaneko, T. Kawaguchi, J. Cryst. Growth 237–239 (2002) 2227–2232.
[15] J. Aaltonen, J. Rantanen, S. Siiriä, M. Karjalainen, A. Jørgensen, N. Laitinen, M. Savolainen, P. Seitavuopio, M. Louhi-Kultanen, J. Yliruusi, Anal. Chem. 75 (2003) 5267–5273.
[16] S. Agatonovic-Kustrin, T. Rades, V. Wu, D. Saville, I.G. Tucker, J. Pharm. Biomed. Anal. 25 (2001) 741–750.
[17] N. Bladgen, R.J. Davey, R. Rowe, R. Roberts, Int. J. Pharm. 172 (2001) 46–52.
[18] N. Bladgen, Powder Technol. 121 (2001) 46–52.
[19] S. Khoskhoo, J. Anwar, J. Phys. Des.: Appl. Phys. 26 (1993) B90–B93.
[20] K. Pöllänen, A. Häkkinen, M. Karjalainen, J. Rantanen, M. Louhi-Kultanen, L. Nyström, Proc. BIWIC, France, 2003, pp. 75–80.
[21] B.G.M. Vandeginste, D.L. Massart, L.M.C. Buydens, S. de Jong, P.J. Lewi, J. Smeyers-Verbeke, Handbook of Chemometrics and Qualimetrics. Part B, Elsevier, Amsterdam, 1998.
[22] A. Höskuldsson, Prediction methods in science and technology, vol. 1 Basic Theory, Colourscan Warsaw Poland, 1996.
[23] S. Wold, H. Antti, F. Lindgren, J. Öhman, Chemom. Intell. Lab. Syst. 44 (1998) 175–185.
[24] T. Fearn, Chemom. Intell. Lab. Syst. 50 (2000) 47–52.
[25] A. Höskuldsson, Chemom. Intell. Lab. Syst. 55 (2001) 23–38.
[26] J.A. Westerhuis, Chemom. Intell. Lab. Syst. 56 (2001) 13–25.
[27] J. Trygg, S. Wold, J. Chemom. 16 (2002) 119–128.
[28] J. Workman, A. Springsteen, Applied Spectroscopy: a Compact Reference for Practitioners, Academic Press, San Diego, CA, 1998.